

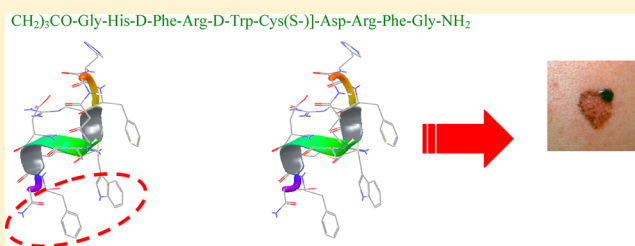
# An Unusual Conformation of $\gamma$ -Melanocyte-Stimulating Hormone Analogues Leads to a Selective Human Melanocortin 1 Receptor Antagonist for Targeting Melanoma Cells

Minying Cai, Magda Stankova,<sup>†</sup> Dhanasekaran Muthu, Alexander Mayorov, Zhehui Yang, Devendra Trivedi, Christopher Cabello, and Victor J. Hruby\*

Department of Chemistry and Biochemistry, 1306 East University Boulevard, University of Arizona, Tucson, Arizona 85721, United States

## S Supporting Information

**ABSTRACT:**  $\gamma$ -MSH ( $\gamma$ -melanocyte-stimulating hormone, H-Tyr-Val-Met-Gly-His-Phe-Arg-Trp-Asp-Arg-Phe-Gly-OH), with its exquisite specificity and potency, has recently created much excitement as a drug lead. However, this peptide is like most peptides susceptible to proteolysis in vivo, which potentially decreases its beneficial activities. In our continued effort to design a proteolytically stable ligand with specific receptor binding, we have engineered peptides by cyclizing  $\gamma$ -MSH using a thioether bridge. A number of novel cyclic truncated  $\gamma$ -MSH analogues were designed and synthesized, in which a thioether bridge was incorporated between a cysteine side chain and an N-terminal bromoacyl group. One of these peptides, cyclo-[(CH<sub>2</sub>)<sub>3</sub>CO-Gly<sup>1</sup>-His<sup>2</sup>-D-Phe<sup>3</sup>-Arg<sup>4</sup>-D-Trp<sup>5</sup>-Cys(S-)]-Asp<sup>7</sup>-Arg<sup>8</sup>-Phe<sup>9</sup>-Gly<sup>10</sup>-NH<sub>2</sub>, demonstrated potent antagonist activity and receptor selectivity for the human melanocortin 1 receptor (hMC1R) (IC<sub>50</sub> = 17 nM). This novel peptide is the most selective antagonist for the hMC1R to date. Further pharmacological studies have shown that this peptide can specifically target melanoma cells. The nuclear magnetic resonance analysis of this peptide in a membrane-like environment revealed a new turn structure, specific to the hMC1R antagonist, at the C-terminus, where the side chain and backbone conformation of D-Trp<sup>5</sup> and Phe<sup>9</sup> of the peptide contribute to hMC1R selectivity. Cyclization strategies represent an approach for stabilizing bioactive peptides while keeping their full potencies and should boost applications of peptide-based drugs in human medicine.



The melanocortin system is involved in numerous physiological functions and may have great potential in novel drug discovery.<sup>1–10</sup> The human melanocortin 1 receptor (hMC1R), mainly present in the periphery, for example, in the skin of mammals, is involved in the control of the relative amounts of pheomelanin and photoprotective eumelanin.<sup>11–13</sup> Appropriate selective hMC1R ligands may offer protection against damaging and mutagenic effects of UV radiation or be useful in the diagnosis and treatment of certain types of skin cancer, such as melanoma. The hMC1R is also present on the surface of various immune cells, macrophages, fibroblasts, monocytes, mast cells, and neutrophils and is a potential target for the development of agents for the treatment of acute and chronic inflammatory diseases, neurodegenerative diseases, and systemic host reactions.<sup>5,11–14</sup> In the central nervous system, the hMC1R is present only on neurons in the periaqueductal gray matter of the midbrain where it is thought to play a role in pain control.<sup>15–17</sup> Despite the multiple physiological functions and the great potential for medical application, there are only a few reports of selective antagonists for the hMC1R available in the literature. Thus, the design of selective hMC1R agonists and antagonists warrants special interest in melanocortin research. Therefore, in our continued effort to produce selective melanocortin ligands, we devoted a great deal of time to obtaining

ligands with selective antagonist activity for the hMC1R and to developing the pharmacological properties that are suitable for medical applications of these compounds.

Structure-based drug design is one of the major strategies in drug discovery.<sup>18–21</sup> In peptide-based drug development, truncations and amino acid scans have been used to find the relevant pharmacophore.<sup>19,22–25</sup> The same method is important for the rational design of melanocortin receptors ligands. Conformational constraints and  $\beta$ -turn mimetics were applied to develop stable and selective melanotropins; the three-dimensional structure of ligands [nuclear magnetic resonance (NMR)] combined with computationally aided drug design helped in the creation of several selective compounds.<sup>26,27</sup> Recently, N-methylation of the amide bonds has been introduced into our novel drug design strategy for identifying the most selective agonist of the hMC1R.<sup>28</sup> In this study, we have designed a selective antagonist of the hMC1R by using a peptide fragment conformation from agouti signaling protein (ASIP)<sup>29</sup> as a template combined with the pharmacophore of  $\gamma$ -MSH. ASIP is

**Received:** August 1, 2012

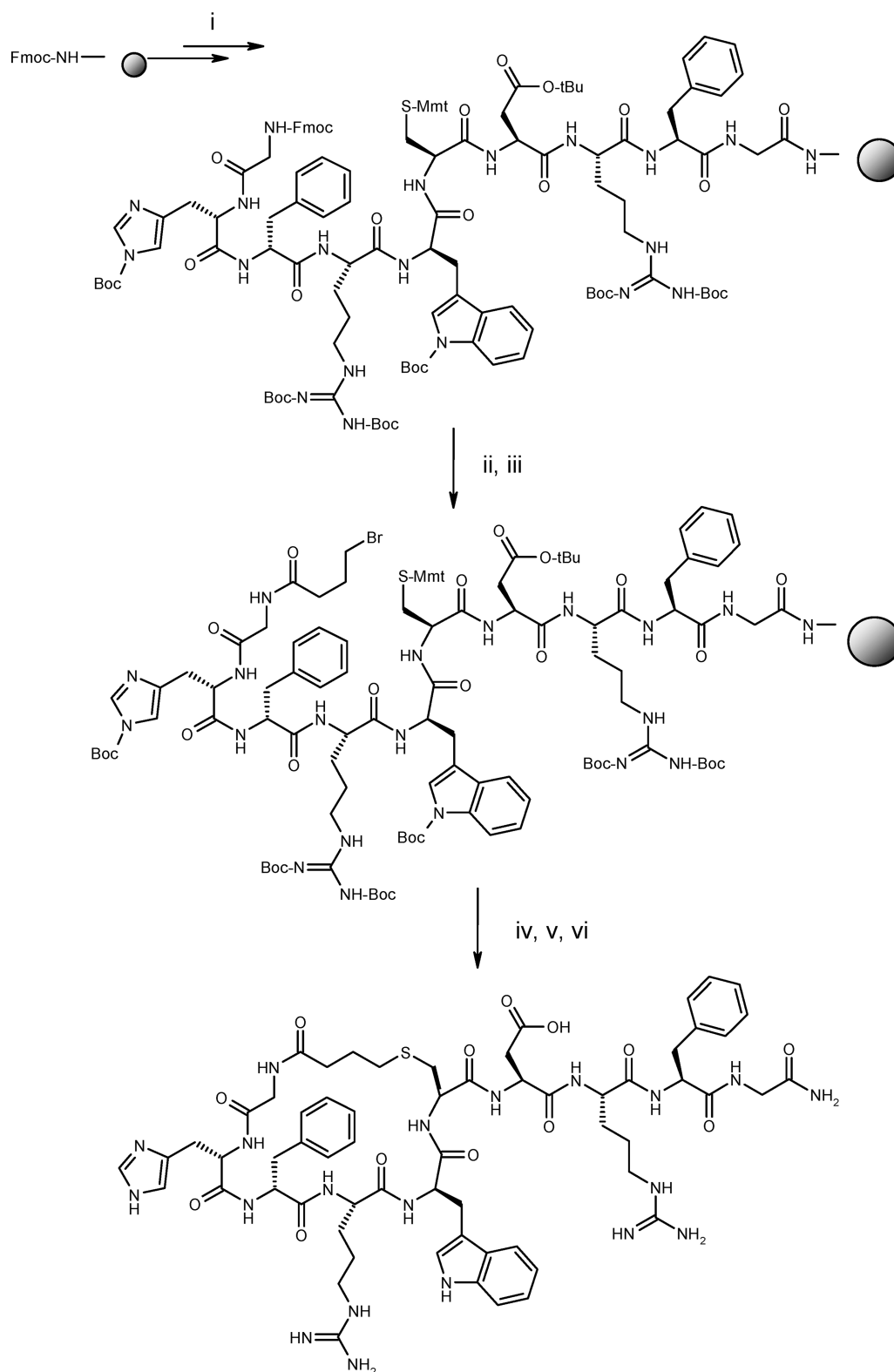
**Revised:** October 15, 2012

**Published:** December 31, 2012





Scheme 1. Synthesis of a Cyclic Analogue of  $\gamma$ -MSH<sup>a</sup>



<sup>a</sup>Reagents: (i) assembly of the linear peptide by the Fmoc strategy; (ii) 20% piperidine in DMF; (iii), 4-bromobutyric acid, DIC, DMF; (iv) 2% TFA/5% Et<sub>3</sub>SiH/CH<sub>2</sub>Cl<sub>2</sub>; (v) 5% DIEA/DMF; (vi) 95% TFA/5% H<sub>2</sub>O.

an endogenous antagonist of the hMC1R. The key feature of the design is a cyclic constraint via a thioether bridge as shown in Scheme 1. Utilizing the thioether bond constraints,  $\gamma$ -MSH leads to improved receptor (subtype) selectivity with enhanced pharmacological and chemical-physical properties, including

metabolic stability, efficacy, lipophilicity, potency, and bioavailability. Further, the newly discovered cyclic hMC1R peptide antagonist also was examined for its conformational properties and tested on melanoma cells to evaluate its potential for in vivo applications.



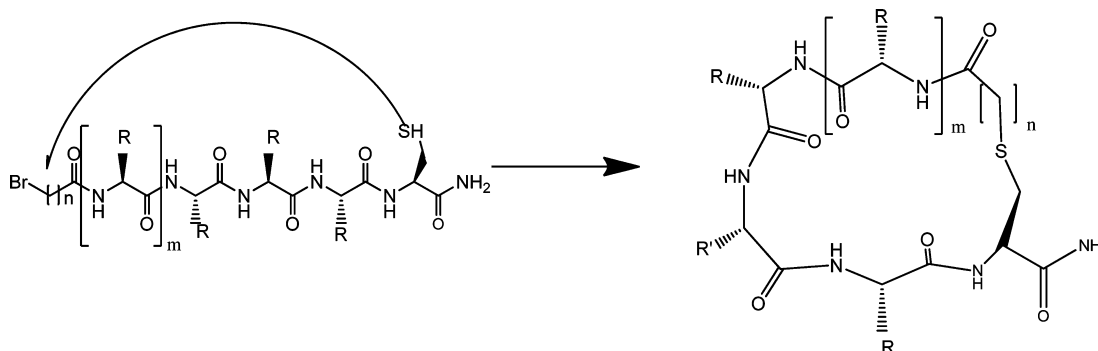


**Figure 1.** General scheme for peptide cyclization using sulfide bridge where  $n = 1, 2$ , or  $3$  and  $m = 1$  or  $2$ .

## DESIGN

The thioether bond has been previously used as a stable disulfide replacement in bioactive cyclic peptides to increase the metabolic stability of peptides.<sup>30–32</sup> The thioether linkage has also been used to prepare conformationally constrained peptides that are analogues of normally linear peptides.<sup>18,30,32–36</sup> Cyclic peptides with thioether bonds have been found in nature, especially in a family of antibiotics and lantibiotics.<sup>37–39</sup>

Thioethers are usually prepared by alkylation of thiols. Thiols are powerful nucleophiles and react with electrophiles in an  $S_N2$  manner to produce thioethers. Nucleophilic substitutions with thiols do not require the use of strong bases and generally proceed at room temperature. In favorable cases, thiol alkylation can even be performed at room temperature in an acidic environment.

We have considered the synthesis of macrocyclic thioethers to be a good way to globally conformationally constrain the natural ligand  $\gamma$ -MSH, because  $\gamma$ -MSH analogues tend to be more selective than  $\alpha$ -MSH from our previous studies.<sup>20</sup> The new ligands were designed to contain an array of rings with 21–23 atoms to form a spectrum of cyclic peptides from less flexible to more flexible analogues. Intramolecular thioether bond formation was proposed to be a good synthetic method for peptide cyclization and a convenient approach for probing peptide conformations. Published data suggest that a 23-membered ring (e.g., MTII, SHU9119)<sup>41–43</sup> is an optimal size for binding of the melanotropin ligand to the melanocortin receptors. So far, the majority of published work is based on  $\alpha$ -MSH cyclic analogues with either lactam or disulfide bridges. The application of thioethers for cyclization of  $\gamma$ -MSH derivatives is a novel structural modification for melanotropin ligands. To form a thioether, we need to introduce a thiol group into a peptide sequence, and one choice for the thiol source was a cysteine residue. The next issue was where to incorporate a cysteine residue into  $\gamma$ -MSH, and for that, we examined two general methods. We can either replace an amino acid with cysteine or insert a cysteine between two amino acids in the natural sequence. Finally, we need to consider a suitable site for an electrophilic moiety. A very simple solution was to apply a bromoacetyl group at the amino terminus of the peptide. We then have two very reactive species, which can form intramolecular thioether-bridged structures (Figure 1). The synthetic procedure is shown in Scheme 1. In this approach, we used bromoacetic acid, 3-bromopropionic acid, and 4-bromobutyric acid to obtain cyclic structures with different ring sizes (Table 1).

**Table 1.** Novel Designed Cyclic  $\gamma$ -MSH Analogues

ligand	sequence	ring size
peptide 1	$c(\text{CH}_2\text{-CO-Gly-His-D-Phe-Arg-Trp-Cys})\text{-Asp-Arg-Phe-Gly-NH}_2$	21
peptide 2	$c(\text{CH}_2\text{-CO-Gly-His-D-Phe-Arg-D-Trp-Cys})\text{-Asp-Arg-Phe-Gly-NH}_2$	21
peptide 3	$c(\text{C}_2\text{H}_4\text{-CO-Gly-His-D-Phe-Arg-Trp-Cys})\text{-Asp-Arg-Phe-Gly-NH}_2$	22
peptide 4	$c(\text{C}_2\text{H}_4\text{-CO-Gly-His-D-Phe-Arg-D-Trp-Cys})\text{-Asp-Arg-Phe-Gly-NH}_2$	22
peptide 5	$c(\text{C}_3\text{H}_6\text{-CO-Gly-His-D-Phe-Arg-Trp-Cys})\text{-Asp-Arg-Phe-Gly-NH}_2$	23
peptide 6	$c(\text{C}_3\text{H}_6\text{-CO-Gly-His-D-Phe-Arg-D-Trp-Cys})\text{-Asp-Arg-Phe-Gly-NH}_2$	23

## EXPERIMENTAL PROCEDURES

$N^\alpha$ -Fmoc amino acids were obtained from Bachem (Torrance, CA), Nova Biochem (Gibbstown, NJ), and AdvancedChem-Tech (Louisville, KY). Fmoc Rink amide resin was purchased from Polymer Laboratories (Santa Clara, CA). Organic solvents and reagents were purchased from Aldrich and used without further purification. All cyclic peptides were synthesized according to a general protocol outlined below.

Rink amide resin (100 mg, 0.065 mmol/g) was placed into a 5 mL polypropylene syringe with the frit on the bottom and swollen in DCM (2 mL) for 30 min and in DMF (2 mL) for 30 min. The Fmoc protecting group on the Rink linker was removed by 50% piperidine in DMF. After 20 min, the solution of piperidine was removed and the resin was washed with DMF (2 mL, 10 times). Fmoc amino acid (3 equiv, 0.195 mmol) and HOBt (3 equiv, 0.195 mmol) were dissolved in 700  $\mu\text{L}$  of DMF, and then DIC (3 equiv, 0.195 mmol) was added. The coupling mixture was transferred into the syringe with the resin and shaken for 1–3 h. The completion of coupling was monitored with bromophenol blue and ninhydrin tests.<sup>40,58</sup> The coupling mixture was removed, and the resin was washed with DMF (2 mL, 5 times). The Fmoc group was cleaved with 50% piperidine in DMF. Each coupling and deprotection step was repeated until a linear peptide was assembled. Bromoacetic acid (3 equiv, 0.195 mmol) was dissolved in 700  $\mu\text{L}$  of DMF, and DIC (3 equiv, 0.195 mmol) was added. The acylation reaction was usually complete after 20 min. The reaction mixture was removed, and the resin was washed with DMF (2 mL, 5 times) and DCM (2 mL, 5 times). The monomethoxytrityl group was cleaved by treatment with a 2% TFA/5% TIPS/DCM mixture (2 mL, 5 times, 5 min for each treatment). The resin was washed with DCM (2 mL, 10 times) and DMF (2 mL, 5 times). Peptide cyclization was performed



**Table 2. Analytical Characterization of Cyclic Peptides 1–6**

peptide	molecular formula	$m/z$ ( $M + H^+$ )		HPLC retention time (min) <sup>a</sup>		TLC $R_f$	
		calcd	observed (ESI)	system I <sup>b</sup>	system II <sup>c</sup>	system I <sup>d</sup>	system I <sup>e</sup>
1	C <sub>60</sub> H <sub>78</sub> N <sub>20</sub> O <sub>13</sub> S	1319.58562	1319.5855	13.71	19.97	0.52	0.17
2	C <sub>60</sub> H <sub>78</sub> N <sub>20</sub> O <sub>13</sub> S	1319.58562	440.5299 <sup>b</sup>	13.14	18.59	0.51	0.15
3	C <sub>61</sub> H <sub>80</sub> N <sub>20</sub> O <sub>13</sub> S	1333.60127	1333.6080	13.45	18.25	0.48	0.13
4	C <sub>61</sub> H <sub>80</sub> N <sub>20</sub> O <sub>13</sub> S	1333.60127	1333.5981	13.09	18.43	0.54	0.20
5	C <sub>62</sub> H <sub>82</sub> N <sub>20</sub> O <sub>13</sub> S	1347.61692	1347.6152	13.86	18.93	0.49	0.13
6	C <sub>62</sub> H <sub>82</sub> N <sub>20</sub> O <sub>13</sub> S	1347.61692	1347.6187	13.47	18.73	0.50	0.13

<sup>a</sup>MS, the theoretical and experimental masses for peptides 1–6 obtained by FT-MS analysis.  $[M + 3H]^{3+}$ . HPLC gradient: 10 to 90% B in A over 40 min, at a flow rate of 1.0 mL/min. <sup>b</sup>Buffer A, 0.1% TFA in H<sub>2</sub>O; buffer B, 0.08% TFA in ACN (pH 3). <sup>c</sup>Buffer A, 20 mM Na<sub>2</sub>HPO<sub>4</sub> in H<sub>2</sub>O; buffer B, 20% H<sub>2</sub>O in ACN (pH 6.3). <sup>d</sup>A 4:2:1:2 *n*-butanol/water/acetic acid/pyridine mixture (pH 6). <sup>e</sup>A 4:1:2 *n*-butanol/water/acetic acid mixture (pH 2.5).

in a solution of 5% DIEA in DMF for 10–12 h at room temperature. The final wash of the resin was conducted with DMF (2 mL, 5 times) and DCM (2 mL, 5 times). The product was cleaved from the resin with a mixture of 95% TFA, 2.5% TIPS, and 2.5% water in 1.5 h. Side chain protecting groups were removed during the cleavage step. The cleavage mixture was evaporated on a rotary evaporator. A crude cyclic peptide was dissolved in acetic acid and purified by HPLC.

TLC was performed using two solvent systems. System I was a 4:2:1:2 *n*-butanol/water/acetic acid/pyridine mixture, and system II was a 4:1:2 *n*-butanol/water/acetic acid mixture. The  $R_f$  values are listed in Table 2.

For HPLC, samples were dissolved in 10–20% methanol in water (1 mg/mL) and 5  $\mu$ L of that solution was injected onto the analytical HPLC column (YMC-Pack ODS-AM, 150 mm  $\times$  4.6 mm, 3  $\mu$ m, 120 Å). Two buffer systems were used for the assessment of peptide purity. Solvent system I consisted of buffer A (0.1% TFA in H<sub>2</sub>O) and buffer B (0.08% TFA in CH<sub>3</sub>CN). Solvent system II consisted of buffer A (20 mM Na<sub>2</sub>HPO<sub>4</sub> in H<sub>2</sub>O) and buffer B (20% CH<sub>3</sub>CN in H<sub>2</sub>O). The retention times ( $t_R$ ) of cyclic peptides are listed in Table 2. Peptide purification was achieved using preparative HPLC. A crude product was dissolved in 50% acetic acid in water (10 mg/mL) and filtered through a minidisk filter, and 1 mL of clear solution was loaded onto the semipreparative column (YMC-Pack ODS-AM, 100 mm  $\times$  10 mm, 5  $\mu$ m, 120 Å). The solvent system for HPLC purification consisted of buffer A (0.1% TFA in H<sub>2</sub>O) and buffer B (0.08% TFA in ACN). The solvent gradient was usually 2% buffer A to 40% buffer B over 15 min with a flow rate of 10 mL/min. Collected fractions of the purified products were lyophilized.

We used high-resolution mass spectrometry for evaluation of molecular formulas of our novel macrocyclic peptide ligands (Table 2). Both ESI and MALDI were used to generate protonated peptides (peptides 1–6). ESI experiments were conducted on an IonSpec 4.7 T Fourier ion cyclotron resonance (ICR) instrument with the peak matching technique by using peptide reference standards. MALDI measurements were taken on a Bruker Reflex III MALDI-TOF instrument.

## BIOLOGICAL ACTIVITY ASSAYS

**Receptor Binding Assays.** Competition binding experiments were conducted using both a cloned cell line and melanoma cells (A375, ATCC). HEK293 cells stably expressing the human MC1 and MC3–MC5 receptors have been described previously.<sup>44,45</sup> HEK293 cells transfected with hMCRs<sup>44,45</sup> were seeded on 96-well plates 48 h before the assay (50000 cells/well). For the assay, the cell culture medium was aspirated and the cells were washed once with a freshly prepared MEM

buffer containing 100% minimum essential medium with Earle's salt (MEM, GIBCO) and 25 mM sodium bicarbonate. Next, the cells were incubated for 40 min at 37 °C with different concentrations of unlabeled peptide and labeled [<sup>125</sup>I]-[Nle<sup>4</sup>, D-Phe<sup>7</sup>]- $\alpha$ -MSH (Perkin-Elmer Life Science, 20000 cpm/well, 33.06 pM) diluted in 125  $\mu$ L of freshly prepared binding buffer containing 100% MEM, 25 mM HEPES (pH 7.4), 0.2% bovine serum albumin, 1 mM 1,10-phenanthroline, 0.5 mg/L leupeptin, and 200 mg/L bacitracin. The assay medium was subsequently removed, and the cells were washed once with basic medium and then lysed by the addition of 10  $\mu$ L of 0.1 M NaOH and 10  $\mu$ L of 1% Triton X-100. The radioactivity of lysed cells was measured by a Wallac MicroBeta TriLux 1450 LSC and luminescence counter (PerkinElmer Life Science, Boston, MA).

**Adenylate Cyclase Assays.** Melanoma and cloned cells were grown to confluence in Dulbecco's modified Eagle's medium (DMEM) and MEM medium (GIBCO), respectively, containing 10% fetal bovine serum, 100 units/mL penicillin and streptomycin, and 1 mM sodium pyruvate. The cells were seeded on 96-well plates 48 h before the assay (50000 cells/well). For the assay, the cell culture medium was removed and the cells were rinsed with 100  $\mu$ L of MEM buffer (GIBCO). An aliquot (100  $\mu$ L) of the Earle's balanced salt solution with 5 nM isobutylmethylxanthine (IBMX) was placed in each well for 1 min at 37 °C. Next, aliquots (25  $\mu$ L) of melanotropin peptides at varying concentrations were added, and the cells were incubated for 3 min at 37 °C. We stopped the reaction by aspirating the assay buffer and adding 60  $\mu$ L of ice-cold Tris/EDTA buffer to each well and then placing the plates in a boiling water bath for 7 min. The cell lysates were then centrifuged for 10 min at 2300g. A 50  $\mu$ L aliquot of the supernatant was transferred to another 96-well plate and placed with 50  $\mu$ L of [<sup>3</sup>H]cAMP and 100  $\mu$ L of protein kinase A (PKA) buffer in an ice bath for 2–3 h. The PKA buffer consisted of Tris/EDTA buffer with 60  $\mu$ g/mL PKA and 0.1% bovine serum albumin by weight. The incubation mixture was filtered through 1.0  $\mu$ m glass fiber filters in MultiScreen-FB 96-well plates (Millipore, Billerica, MA). The total amount of [<sup>3</sup>H]cAMP was measured by a Wallac MicroBeta TriLux 1450 LSC and luminescence counter (PerkinElmer Life Science). The cAMP accumulation data for each peptide analogue were determined with the help of a cAMP standard curve generated by the same method as described above. IC<sub>50</sub> and EC<sub>50</sub> values represent the means of two experiments performed in triplicate. IC<sub>50</sub> and EC<sub>50</sub> values and their associated standard errors were determined for binding and cAMP assays by fitting the data using a nonlinear least-squares analysis, with the help of GraphPad Prism 4 (GraphPad Software, San Diego, CA). The maximal amount of cAMP produced with each ligand at 10  $\mu$ M was compared to



Table 3. Binding and cAMP Assays of Novel Cyclized Peptides toward Human Melanocortin Receptors<sup>a</sup>

	hMC1R			hMC3R			hMC4R			hMCSR		
	IC <sub>50</sub> (nM)	EC <sub>50</sub> (nM)	Act%	IC <sub>50</sub> (nM)	EC <sub>50</sub> (nM)	Act%	IC <sub>50</sub> (nM)	EC <sub>50</sub> (nM)	Act%	IC <sub>50</sub> (nM)	EC <sub>50</sub> (nM)	Act%
1	2000	>1000	/	1630 ± 300	195 ± 23	140	NB	800 ± 90	37	510 ± 60	86 ± 10	31
2	1800	NA	/	NB	>1000	30	NB	NA	/	NB	>1000	0
3	330 ± 60	NA	10	76 ± 10	170 ± 30	52	NB	NA	/	160 ± 20	2500	100
4	30 ± 4	NA	/	17000	1100 ± 120	50	NB	NA	NA	115 ± 10	1000	0
5	29 ± 3	NA	/	8500	100 ± 14	50	NB	NA	/	210 ± 30	873 ± 100	91
6	17 ± 2	NA	/	3900	59 ± 6	75	NB	NA	/	1000 ± 110	1300	65
[Nle <sup>3</sup> ]-γ-MSH	60 ± 5	80 ± 7	100	62 ± 8	1000 ± 100	100	45 ± 5	70 ± 7	100	640 ± 100	82 ± 8	100
[Nle <sup>3</sup> ]-γ-MSH-NH <sub>2</sub>	—	—	—	45 ± 7	1.6 ± 0.2	100	64 ± 7	34 ± 4	105	200 ± 23	99 ± 10	114
γ-MSH	1000 ± 20	300 ± 30	100	71 ± 10	700 ± 89	100	760 ± 80	710 ± 70	100	2200 ± 200	550 ± 60	100

<sup>a</sup>IC<sub>50</sub> is the concentration of peptide at 50% specific binding (*N* = 4). NB means that 0% of [<sup>125</sup>I]NDP-α-MSH displacement was observed at 10 μM. EC<sub>50</sub> is the effective concentration of peptide that was able to generate 50% maximal intracellular cAMP accumulation (*N* = 4). Act% is the percentage of cAMP produced at a ligand concentration of 10 μM, in relation to MT-II. NA indicates 0% cAMP accumulation observed at 10 μM. The peptides were tested over a range of concentrations from 10<sup>-10</sup> to 10<sup>-5</sup> M.

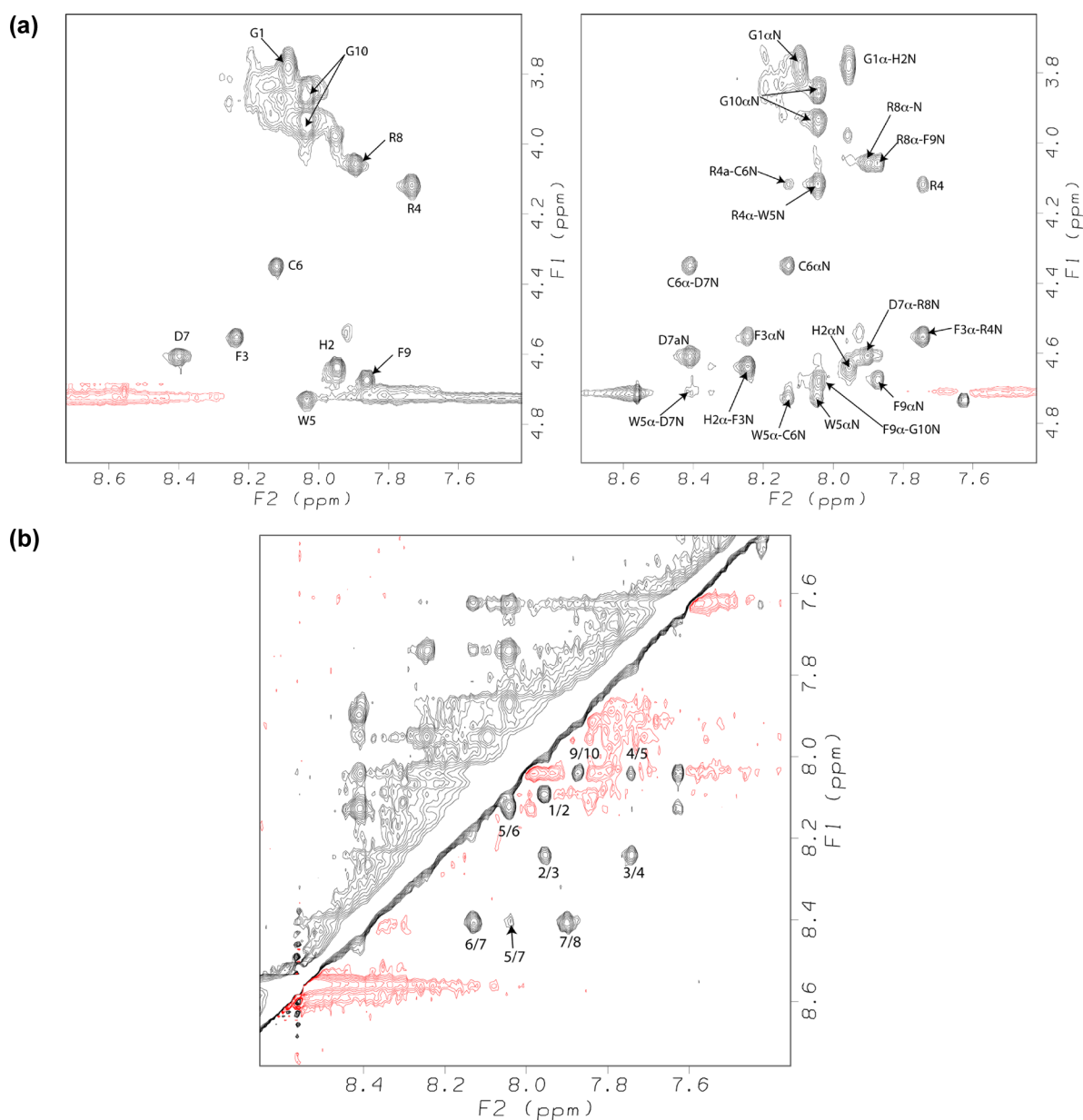
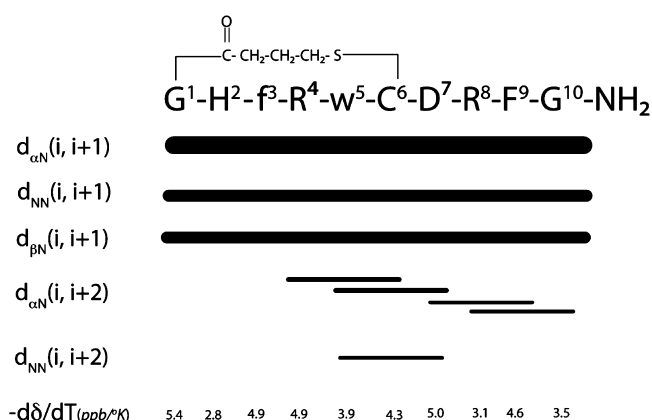


Figure 2. (a) Fingerprint regions of TOCSY (left) and NOESY (right) spectra of peptide 6. (b) Amide (NH–NH) region of the NOESY spectrum showing sequential  $d_{NN}(i, i + 1)$  NOEs of peptide 6.



**Table 4. Chemical Shift Values (parts per million) of Peptide 6 As Measured in SDS Micelles at a Concentration of 6.11 mM, pH 5.5, and 25 °C**

residue	NH	C <sup>α</sup> H	C <sup>β</sup> H	Δδ (ppm)	dδ/dT (−ppb/K)
Gly <sup>1</sup>	8.088	3.782		−0.228	5.40
His <sup>2</sup>	7.946	4.637		−0.133	2.82
Phe <sup>3</sup>	8.235	4.551	2.922 3.097	−0.069	4.90
Arg <sup>4</sup>	7.734	4.118		−0.222	4.94
Trp <sup>5</sup>	8.034	4.729	3.243 3.455	0.059	3.88
Cys <sup>6</sup>	8.120	4.348	2.847 2.972	−0.232	4.26
Asp <sup>7</sup>	8.398	4.606	2.979 2.860	−0.024	5.02
Arg <sup>8</sup>	7.894	4.057		−0.283	3.08
Phe <sup>9</sup>	7.862	4.675	2.976 3.291	0.055	4.64
Gly <sup>10</sup>	8.039	3.866 3.949		−0.103	3.54



**Figure 3.** Summary of observed NOEs and temperature coefficient values measured for peptide 6 in SDS micelles at 25 °C and pH 5.5. Lowercase letters denotes D-amino acids. The thickness of the lines is approximately proportional to the intensity of the NOE cross-peaks.

the amount of cAMP produced with standard agonist MT-II at 10  $\mu$ M and is expressed in percent (as % max effect) in Table 3. The  $pA_2$  is 8.1.

**Data Analysis.** IC<sub>50</sub> and EC<sub>50</sub> values represent the means of two experiments performed in triplicate. IC<sub>50</sub> and EC<sub>50</sub> estimates and their associated standard errors were determined

by fitting the data using a nonlinear least-squares analysis, with the help of GraphPad Prism 4 (GraphPad Software).

**NMR Spectroscopy Methods.** All NMR spectra were recorded on a Bruker DRX600 600 MHz spectrometer at 298 K. The peptide concentration for the NMR experiments was 4.7 mM. The micelle samples were prepared by dissolving the peptide and 50 equiv of perdeuterated SDS in 0.6 mL of acetate buffer (10 mM) containing 10% D<sub>2</sub>O. The pH of the each sample was adjusted to 5.5 by using DCl or NaOD as necessary. Deuterated 3-(trimethylsilyl)propionic acid (TSP) was added as an internal standard for referencing. Two-dimensional nuclear Overhauser enhancement (NOESY) and total correlation (TOCSY) spectra were acquired using standard pulse sequences and processed using XWINNMR (Bruker Inc.) and FELIX2000 (Accelrys Inc., San Diego, CA). Mixing times for TOCSY spectra were 60 ms and for NOESY spectra 300 ms. All experiments included 750 increments in  $t_1$ , 16 or 32 scans each, with a 1.5 s relaxation delay and a size of 2K or 4K, and spectral processing was achieved with shifted sine bell window multiplications in both dimensions. Water suppression was achieved by using the WATERGATE pulse sequence. Coupling constants ( $^3J_{\alpha H-NH}$ ) were measured from the DQF-COSY spectrum.

**Structure Calculation Methods.** Distance constraints for the structure calculation were obtained from integral volumes of the NOESY peaks. The NOE integral volumes were classified as strong, medium, and weak with 3.0, 4.0, and 5.0 Å, respectively, as upper bound distances. Molecular dynamics simulation was conducted with the INSIGHT/DISCOVER package (Accelrys Inc.) with a consistent valency force field (CVFF). All the calculations were conducted in vacuo. A distance-dependent dielectric constant (2.5 $r$ , where  $r$  is the distance in angstroms) was used. All peptide bonds were constrained to the trans conformation by a 100 kcal mol<sup>−1</sup> energetic penalty. Distance restraints with a force constant of 25 kcal mol<sup>−1</sup> were applied in the form of a flat-bottom potential well with a common lower bound of 1.8 Å and upper bounds of 3.0, 4.0, and 5.0 Å in accordance with observed weak, moderate, and strong NOE intensities, respectively. Only the distance restraints from inter-residue NOEs were included in the calculation. Dihedral angle restraints based on the C<sup>α</sup>H chemical shift index (CSI) were imposed on the residues displaying negative deviation. Thus, for a CSI of greater than −0.10 ppm, the  $\phi$  and  $\psi$  restraints were in the range of −90° to −30° and −60° to 0°, respectively, while for a CSI of at most −0.10 ppm, the corresponding ranges were −150° to −30° for  $\phi$  and −90° to 150° for  $\psi$ . For D-chiral amino acids, the opposite dihedral angle values were used.

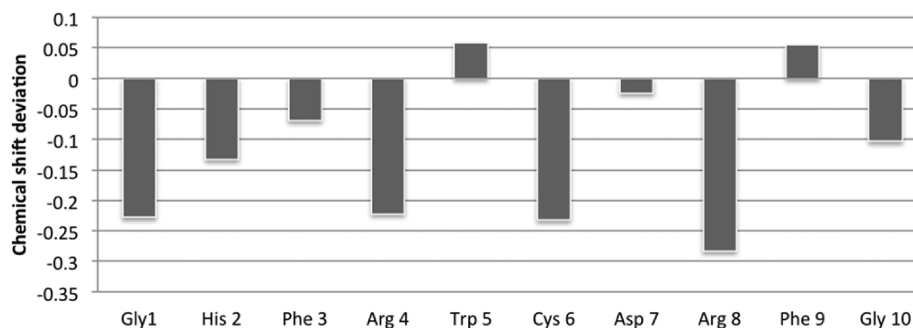


**Figure 4.** Chemical shift deviations of C<sup>α</sup>H chemical shift values from random coil values.



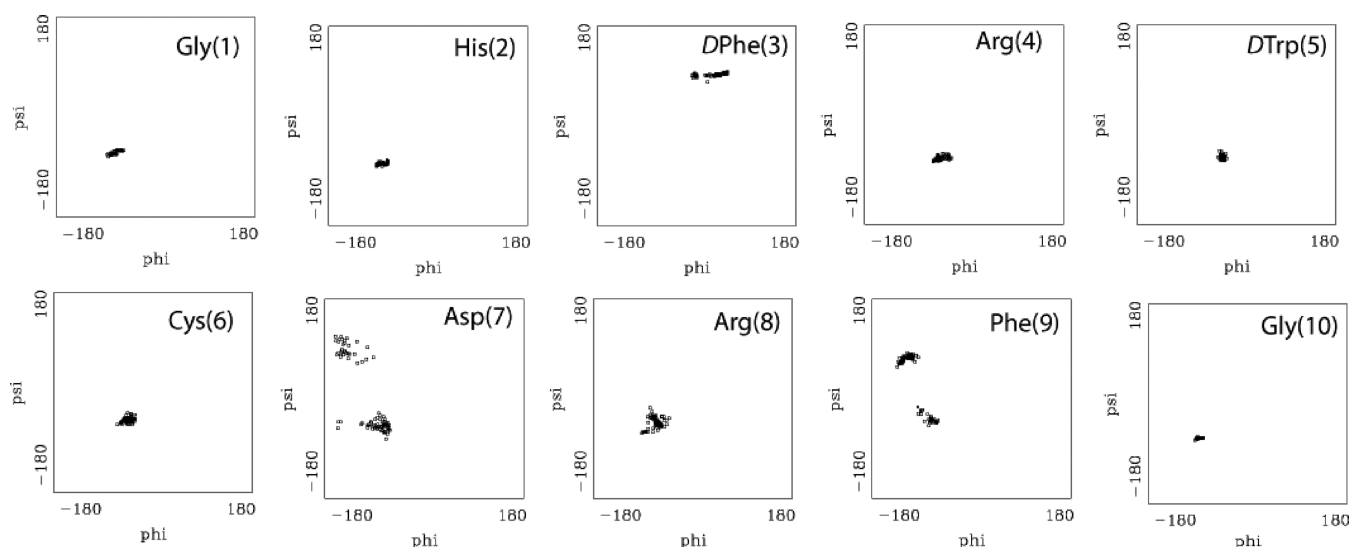


**Figure 5.**  $\phi$  and  $\psi$  dihedral angle distribution (i.e., Ramachandran plot) of each amino acid in peptide 6 for the resultant 100 structures from the simulated annealing molecular dynamics calculations.

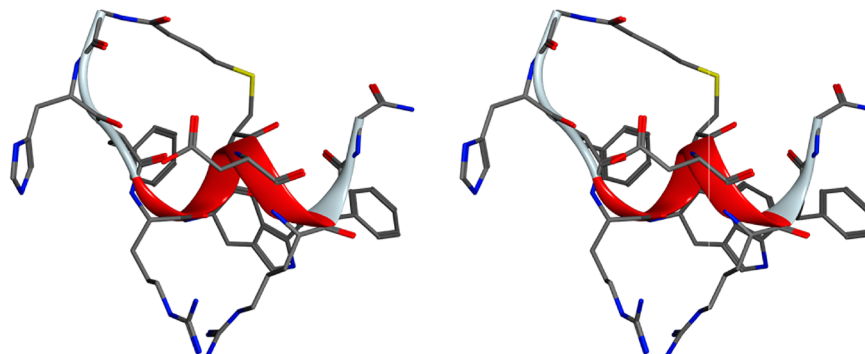


**Figure 6.** Stereoview of the lowest-energy structure from the simulated annealing molecular dynamics calculations of peptide 6. The hydrogen atoms are not shown for the sake of clarity. The ribbon diagram shows the secondary structure of the peptide.

## RESULTS AND DISCUSSION

**Bioassay Results.** It has been shown that D-phenylalanine is a critical amino acid in the tetrapeptide (Pharmacophore) sequence of  $\gamma$ -MSH for enhancing potency, whereas a D-tryptophan improves selectivity.<sup>41–47</sup> We have prepared three peptides with the same sequence containing D-Phe, but with different ring sizes (peptides 1, 3, and 5), and three other peptides that have D-Phe and D-Trp (peptides 2, 4, and 6) (Table 1) in their sequences with systematic differences in the size of their rings. The binding affinities and the in vitro cAMP accumulation data for these analogues are summarized in Table 3. Analogue 1 with a 21-membered ring was found to be a very weak antagonist ( $IC_{50}$  = 2000 nM) at the hMC1R, a full agonist at the hMC3R ( $EC_{50}$  = 190 nM), inactive at the hMC4R, and a partial agonist at the hMC5R ( $EC_{50}$  = 86 nM; 31% activation). Similar observations were made with analogue 2, which also has a 21-membered ring. This analogue exhibited weak antagonist activity ( $IC_{50}$  = 1800 nM) at the hMC1R and was inactive at the hMC3R, hMC4R, and hMC5R. It is interesting to note that peptide 2 that has a D-Trp residue, though not potent at the hMC1R, is nonetheless very selective. For analogues 3 and 4, the ring size was increased by one carbon atom to 22, and this improves binding affinity. Analogue 3 had partial antagonist activity toward the hMC3R ( $IC_{50}$  = 76 nM; 52% activation). Also, this analogue was found to have no binding to the hMC4R

**Table 5.**  $\phi$  and  $\psi$  Angle Distribution of Peptide 6 from a Simulated Annealing Molecular Dynamics Study<sup>a</sup>

amino acid	all 100 structures		lowest-energy structure	
	$\phi$	$\psi$	$\phi$	$\psi$
Gly <sup>1</sup>	−72(7)	−64(3)	−75	−67
His <sup>2</sup>	−83(7)	−68(2)	−91	−69
D-Phe <sup>3</sup>	34(21)	92(2)	34	90
Arg <sup>4</sup>	−47(8)	−60(3)	−55	−65
D-Trp <sup>5</sup>	−26(3)	−60(3)	−28	−61
Cys <sup>6</sup>	−42(7)	−50(4)	−49	−46
Asp <sup>7</sup>	−87(33)	−45(65)	−70	−59
Arg <sup>8</sup>	−66(9)	−43(9)	−68	−33
Phe <sup>9</sup>	−107(21)	70(52)	−116	82
Gly <sup>10</sup>	−88(3)	−62(1)	−82	−62

<sup>a</sup>The standard deviation from the average value is given in parentheses, and deviations of >30 are shown in bold.

and to be a full but weak agonist at the hMC5R ( $EC_{50}$  = 2500 nM). Analogue 4 in which Trp was replaced with D-Trp had much improved binding affinity for the hMC1R ( $IC_{50}$  = 30 nM) with no cAMP accumulation activity (antagonist). This analogue was found to be a very weak partial agonist ( $EC_{50}$  = 1100 nM; 50% activation) at the hMC3R, to have modest antagonist activity at the hMC5R, and to be totally inactive toward the hMC4R.



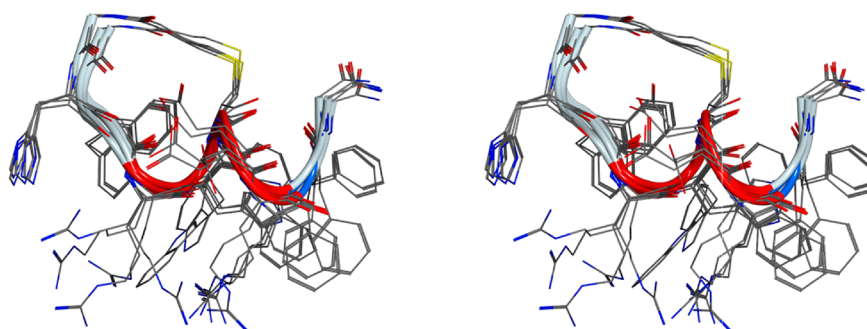


**Figure 7.** Stereoview of an overlay of the five lowest-energy structures resulting from the simulated annealing molecular dynamics calculations of peptide 6. The hydrogen atoms are not shown for the sake of clarity. The ribbon diagram shows the secondary structure of the peptide.

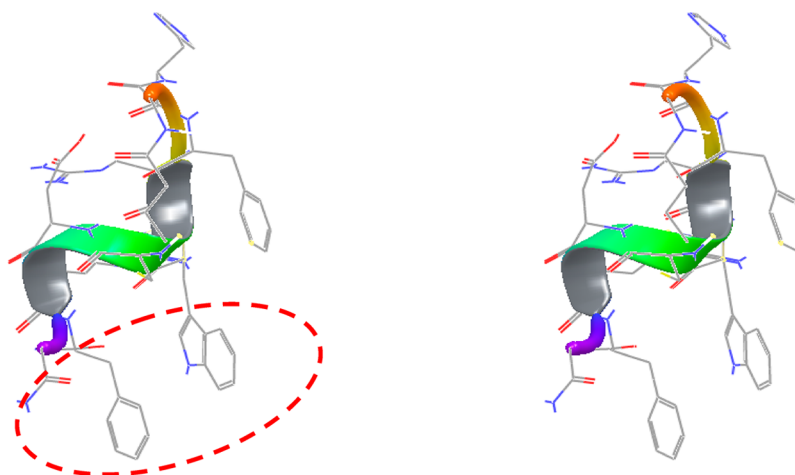


**Figure 8.** Stereoview of the lowest-energy structure showing the new binding site of peptide 6 with the dashed oval.

Analogue 5 was very similar to analogue 4 with antagonist activity at the hMC1R ( $IC_{50} = 29$  nM) but with partial agonist activity at the hMC3R ( $EC_{50} = 100$  nM). This analogue was inactive at the hMC4R but exhibited full agonist activity toward the hMC5R (91% activation). Analogue 6 (Table 3) was the most interesting analogue in this series. It demonstrated potent antagonist activity for the hMC1R ( $IC_{50} = 17$  nM). This analogue was inactive at the hMC4R and was a very weak partial agonist at the hMC3R ( $EC_{50} = 3900$  nM; 75% activation) and weak partial agonist at the hMC5R ( $EC_{50} = 1300$ ; 65% activation). It is interesting to note that hMC1R selectivity is very much dependent on the conformational constraint. Thus, cyclic analogues of  $\gamma$ -MSH obtained by incorporating a thioether bridge between a cysteine side chain and an N-terminal bromoacyl group were found to be very critical in forming the right conformation constraint for selectivity, and in this study, the 23-membered ring was most favorable for hMC1R selectivity (peptide 6).

**NMR Studies.** To explore the conformation underlying the selective antagonist activity of the hMC1R, we have analyzed the structure of peptide 6 using NMR conformational studies.

The spin system of each amino acid present in the peptide was identified using TOCSY spectra. This information was used with NOESY spectra to determine the sequential assignment of the peptide. The fingerprint regions of the TOCSY and NOESY spectra are shown in Figure 2.  $d_{\alpha N}(i, i + 1)$  and  $d_{\beta N}(i, i + 1)$  were helpful in unambiguous sequential assignment of the peptide. The chemical shift values along with  $^3J_{\alpha NH}$  and temperature coefficient values are listed in Table 4. The observed NOEs are summarized in Figure 3. The peptide displayed strong sequential  $d_{\alpha N}(i, i + 1)$  and  $d_{\beta N}(i, i + 1)$  NOEs throughout

the sequence along with relatively weaker  $d_{NN}(i, i + 1)$  NOEs. The observation of strong consecutive  $d_{\alpha N}(i, i + 1)$  and relatively weaker  $d_{NN}(i, i + 1)$  NOEs suggests that the peptide undergoes rapid interconversion between extended and folded conformations.<sup>48,49</sup> The absence of helix diagnostic  $d_{\alpha N}(i, i + 3)$  and  $d_{\alpha N}(i, i + 4)$  NOEs and the observation of four  $d_{\alpha N}(i, i + 2)$  NOEs and one  $d_{NN}(i, i + 2)$  NOE suggest multiple turns or a  $3_{10}$ -type helical region in the middle segment of the peptide.

The hydrogen bond information about the peptide can be obtained from the temperature coefficient ( $d\delta/dT$ ) values of the amide protons.<sup>50</sup> The temperature coefficient values were obtained by recording the TOCSY spectrum at different temperatures with 5 °C increments starting from 20 °C because the one-dimensional proton NMR spectrum showed a large amount of overcrowding in the amide proton region. The observation of diminished temperature coefficient values (i.e., less than  $-4$  ppb/K) for amide protons of His<sup>5</sup>, Trp<sup>8</sup>, Arg<sup>11</sup>, and Gly<sup>12</sup> indicates that those amide protons are involved in hydrogen bonding or are shielded from the solvent, whereas the other amide protons are exposed to solvent.

It is possible to obtain qualitative structural information from  $C^\alpha H$  chemical shift values as they are sensitive to the secondary structure of the peptide.<sup>51</sup> It is well established that consecutive negative deviations of  $C^\alpha H$  chemical shift values from random coil values indicate a helical fold and a positive deviation indicates a  $\beta$ -sheet structure. The chemical deviation plot (also known as a CSI plot) is shown in Figure 4. A negative deviation was observed for all the residues with interruptions at Trp<sup>8</sup> and Phe<sup>11</sup>, suggesting that the residues at the N-terminus possibly have conformational preferences in the helical domain. The positive



deviation at Trp<sup>8</sup> and Phe<sup>11</sup> implies a turn-type fold around those residues.

**Structure Calculations.** To obtain the three-dimensional structure of peptide **6**, we conducted a simulated annealing molecular dynamics calculation by applying distance as well as dihedral angle constraints as described in Experimental Procedures. The stereochemical quality of the final energy-minimized structures from the calculation was checked by the distribution of backbone dihedral angles  $\phi$  and  $\psi$  in the Ramachandran plot<sup>52</sup> as shown in Figure 5. The distribution range is very narrow for all the amino acids except Asp<sup>7</sup> and Phe<sup>9</sup>. This clearly suggests that all the residues except Asp<sup>7</sup> and Phe<sup>9</sup> are in a rigid conformation. Two distinct populations, namely extended and helical, are experienced by Asp<sup>7</sup> and Phe<sup>9</sup>. Interestingly, the dihedral space for D-Trp<sup>5</sup> falls in the negative quadrant of the Ramachandran plot, which is unexpected for a D-amino acid. The same result was obtained even after the calculation was repeated with strong chiral constraints in place. This may be due to the global constraint introduced by the cyclization.

The lowest-energy structure is shown in Figure 6. Consecutive type III  $\beta$ -turns are observed for the -Arg<sup>4</sup>-D-Trp<sup>5</sup>-Cys<sup>6</sup>-Asp<sup>7</sup>-Arg<sup>8</sup>- middle segment as indicated by the consecutive  $d_{\alpha N}(i, i + 2)$  NOEs in this region. As the  $3_{10}$ -type helical dihedral angle values are similar to single type III  $\beta$ -turn dihedral values ( $\phi = -60^\circ$ , and  $\psi = -30^\circ$ ), this region containing consecutive turns can be described as a  $3_{10}$ -helical region. Both termini are flexible in nature despite the cyclization. Previous NMR analysis of shorter analogues related to  $\alpha$ -MSH suggested a  $\beta$ -turn-like structure at -His<sup>6</sup>-D-Phe<sup>7</sup>-Arg<sup>8</sup>-Trp<sup>9</sup>, but the exact type and position of the  $\beta$ -turn depended on the nature of the amino acid substitution in the core pharmacophore region.<sup>53</sup> The main difference between the peptide discussed here and those peptides is the C-terminal extension of four additional residues. The C-terminal extension was favorable for the formation of consecutive  $\beta$ -turns, i.e., the short  $3_{10}$ -helical-type fold. This conformation implies that the C-terminus of the peptide could be a new binding site. The analysis of the backbone dihedral angle values is given in Table 5. An overlay of the five lowest-energy structures from the calculation is shown in Figure 7. The backbone atoms aligned very well, but the side chains of all the amino acids except His<sup>2</sup> are flexible. This observation parallels our earlier studies in which the His residue in cyclized peptides can be replaced with different constrained amino acids without interfering with the binding.<sup>54</sup> The stereoview of the potential new binding site of peptide **6** is shown in Figure 8.

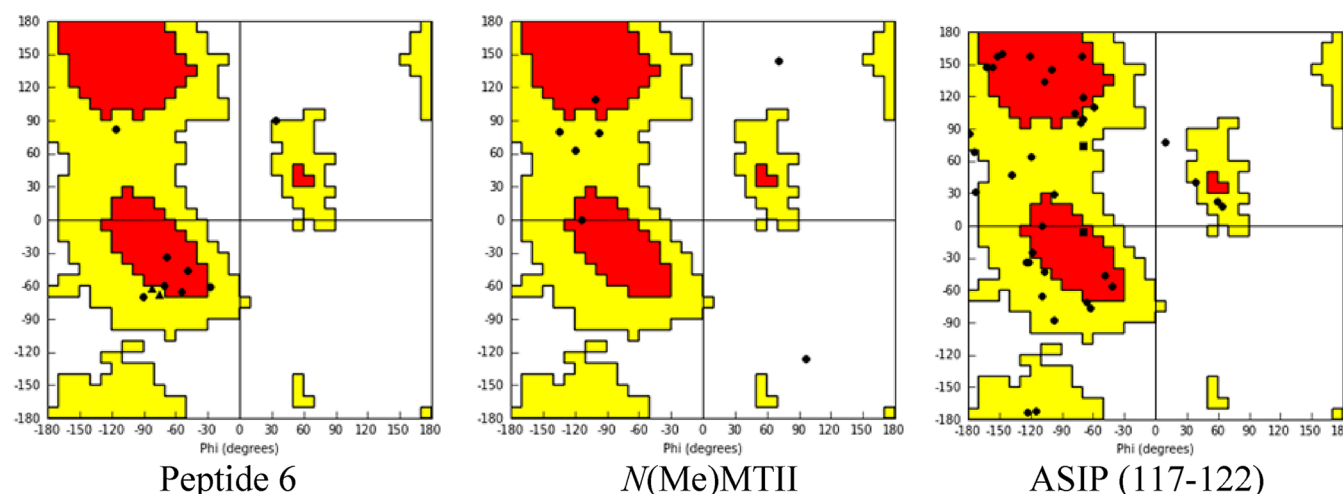
To further explore the structural features of the hMC1R antagonist selectivity of peptide **6**, we have systematically compared the backbone and side chain conformations of peptide **6** with a recently reported selective hMC1R agonist<sup>28</sup> as well as the selective endogenous hMC1R antagonist agouti signal protein, ASIP (Protein Data Bank entry 2KZA),<sup>55</sup> in detail. The compared dihedral angles are listed in Table 6. It is interesting to note that the backbone dihedral angles of the lowest-energy conformation of peptide **6** for -D-Trp<sup>5</sup>-Cys<sup>6</sup>-Asp<sup>7</sup>-Arg<sup>8</sup>-Phe<sup>9</sup>-Gly<sup>10</sup>- matched those of the NMR-derived pharmacophore of ASIP(117–122), -Arg<sup>117</sup>-Phe<sup>118</sup>-Phe<sup>119</sup>-Arg<sup>120</sup>-Ser<sup>121</sup>-Ala<sup>122</sup>- (Table 6), except for the pair of Asp<sup>47</sup> and Arg<sup>120</sup>. These dihedral angle data demonstrate that the backbone conformations of ASIP(117–122) and the C-terminus of peptide **6** are similar. This observation implies that there is a new binding site for peptide **6** in the region of -D-Trp<sup>5</sup>-Cys<sup>6</sup>-Asp<sup>7</sup>-Arg<sup>8</sup>-Phe<sup>9</sup>-Gly<sup>10</sup>- instead of -His-D-Phe-Arg-Trp-. This result is consistent

Table 6. Comparison of the Pharmacophore of the NMR Structures of NMe-MTII, Peptide **6**, and ASIP(117–122)<sup>a</sup>

	Nle <sup>3</sup>		Asp <sup>4</sup> /Gly <sup>1</sup>		His <sup>5</sup> /His <sup>2</sup>		D-Phe <sup>6</sup> /D-Phe <sup>3</sup>		Arg <sup>7</sup> /Arg <sup>4</sup> /Arg <sup>117</sup>		Trp <sup>8</sup> /D-Trp <sup>5</sup> /Phe <sup>118</sup>		Lys <sup>9</sup> /Cys <sup>6</sup> /Phe <sup>119</sup>		Asp <sup>7</sup> /Arg <sup>120</sup>		Arg <sup>8</sup> /Ser <sup>121</sup>		Phe <sup>9</sup> /Ala <sup>122</sup>	
	$\phi$	$\psi$	$\phi$	$\psi$	$\phi$	$\psi$	$\phi$	$\psi$	$\phi$	$\psi$	$\phi$	$\psi$	$\phi$	$\psi$	$\phi$	$\psi$	$\phi$	$\psi$	$\phi$	$\psi$
NMe-MTII	-101	109.1	71.4	143.7	-97.8	78.4	96.1	-125.9	-135.2	80.4	-119.8	62.6	-113.7	0.4	-70.3	-59.5	-68.4	-33.5	-115.6	82.0
peptide <b>6</b>			-75.3	-67.3	-90.9	-69.5	34.1	90.1	-54.8	-64.8	-28.4	-61.1	-45.8	-45.8	-70.3	-59.5	-68.4	-33.5	-115.6	82.0
ASIP(117–122)									-115.4	-171.7	-41.4	-56.5	-48.8	-45.9	63.5	18.4	-118.2	-24.5	-119.5	64.6

<sup>a</sup>Backbone torsion angles (degrees) for the NMR structures of the peptide backbone conformation.  $\alpha$ -MSH analogues are shown in italics (NMe-MTII {Ac-Nle<sup>3</sup>-c[NMe-Asp<sup>4</sup>-NMe-His<sup>5</sup>-D-Phe<sup>6</sup>-NMe-Arg<sup>7</sup>-NMe-Trp<sup>8</sup>-Lys<sup>9</sup>]-NH<sub>2</sub>}), bold (peptide **6** {cyclo-[(CH<sub>2</sub>)<sub>3</sub>CO-Gly<sup>1</sup>-His<sup>2</sup>-D-Phe<sup>3</sup>-Arg<sup>4</sup>-D-Trp<sup>5</sup>-Cys<sup>6</sup>-(S)-<sup>6</sup>]-Asp<sup>7</sup>-Arg<sup>8</sup>-Phe<sup>9</sup>-Gly<sup>10</sup>-NH<sub>2</sub>}), and bold and italics [ASIP loop (-Arg<sup>117</sup>-Phe<sup>118</sup>-Phe<sup>119</sup>-Arg<sup>120</sup>-Ser<sup>121</sup>-Ala<sup>122</sup>-)].





**Figure 9.** Ramachandran Plot of the lowest-energy conformation of the selective antagonist of the hMC1R (peptide 6) and hMC1R selective agonist NMe-MTII and ASIP(117–122).

**Table 7. Binding and cAMP Activities of Peptide 6 with Human Melanoma Cells (A375)<sup>a</sup>**

compound	structure	IC <sub>50</sub>	binding efficiency	EC <sub>50</sub>	Act%
peptide 6	c[(CH <sub>2</sub> ) <sub>3</sub> -Gly-His-D-Phe-Arg-D-Trp-Cys(S-)]-Asp-Arg-Phe-Gly-NH <sub>2</sub>	92 ± 65	98 ± 41	22 ± 2.5	NA
MT-II	Ac-Nle-c[Asp-His-D-Phe-Arg-Trp-Lys]-NH <sub>2</sub>	6.7 ± 2.9	100 ± 10	110 ± 0.6	100
SHU9119	Ac-Nle-c[Asp-His-D-Nal(2')-Arg-Trp-Lys]-NH <sub>2</sub>	100 ± 96	80 ± 34	3.3 ± 2.6	NA

<sup>a</sup>IC<sub>50</sub> is the concentration of peptide at 50% specific binding (*N* = 4). Binding efficiency is the maximal percentage of [<sup>125</sup>I]NDP- $\alpha$ -MSH displacement observed at 10  $\mu$ M. EC<sub>50</sub> is the effective concentration of peptide that was able to generate 50% maximal intracellular cAMP accumulation (*N* = 4). Act% is the percentage of cAMP produced at a ligand concentration of 10  $\mu$ M, in relation to MT-II. NA means 0% cAMP accumulation was observed at 10  $\mu$ M. The peptides were tested over a range of concentrations from 10<sup>-10</sup> to 10<sup>-5</sup> M.

with our earlier work<sup>47</sup> that showed that a new binding site was observed on the basis of the SAR study of  $\gamma$ -MSH. Comparing the backbone dihedral angles of hMC1R agonist NMe-MTII<sup>28</sup> and peptide 6, one can see that the major difference is at D-Trp<sup>5</sup> (peptide 6) versus Trp<sup>8</sup> (NMe-MTII). Both the  $\phi$  and  $\psi$  angles of D-Trp<sup>5</sup>/Trp<sup>8</sup> have a difference of 90–180°. Therefore, we conclude that the conformation of D-Trp<sup>5</sup>/Trp<sup>8</sup> in MSHs is critical for selective agonist/antagonist activity at the hMC1R. Comparison of the Ramachandran plots of peptide 6, NMe-MTII, and ASIP(117–122) (Figure 9) shows the critical conformational properties of constrained peptide 6. The D-Trp configuration falls in the negative quadrant of the Ramachandran plot, which is unusual for a  $\delta$ -amino acid because of the topographic constraint, but that is not true in the case of NMe-MTII. The Ramachandran plot of ASIP has dihedral angles on both sides of the L- and D-like configuration, even though there is no D-amino acid in this natural protein. The D-like configuration of Phe in the ASIP protein is confined by the disulfide bond and the topographic constraint via the whole protein. Thus, the topographic constraint of ASIP(117–122) directs Phe to play its role in hMC1R antagonist selectivity. This SAR study is an example of conformationally based ligand design that may be generally useful in peptide drug design.

**Biological Activity at the Melanoma Cancer Cells.** To further investigate the potential application of peptide 6 toward melanoma cells, we conducted both binding and cAMP assays using the A375 melanoma cell lines (ATCC). Table 7 shows that peptide 6 binds to the melanoma cell receptor in the nanomolar range. It is interesting to note that peptide 6 and SHU9119 act as antagonists toward the melanoma cells. On the other hand, MTII kept its agonist activity, but the cAMP efficacy (EC<sub>50</sub>) is reduced by 2 orders of magnitude compared

to that of the cloned hMC1R cells. This may be due to the lower density of the hMC1R in the cancer cell line. Peptide 6 is an excellent probe for targeting specifically melanoma cells for skin cancer diagnosis and treatment in the future. This observation is consistent with the latest report of ASIP that a lack of natural antagonist of the hMC1R (ASIP) will increase the risk of melanoma, and ASIP pigmentation variants are associated with cutaneous melanoma and basal cell carcinoma.<sup>57</sup> The new result can also explain why the conformation of peptide 6 for -D-Trp<sup>5</sup>-Cys<sup>6</sup>-Asp<sup>7</sup>-Arg<sup>8</sup>-Phe<sup>9</sup>-Gly<sup>10</sup>- matched very well with the NMR-derived pharmacophore of ASIP(117–122), -Arg<sup>117</sup>-Phe<sup>118</sup>-Phe<sup>119</sup>-Arg<sup>120</sup>-Ser<sup>121</sup>-Ala<sup>122</sup>.

In summary, structure–activity relationships (SARs) of cyclic  $\gamma$ -MSH analogues were examined to evaluate the multiple factors that contribute to melanocortin 1 receptor selectivity and are illustrated by Figures 2–9 and Tables 2–6. Figures 8 and 9 illustrate the new binding site of  $\gamma$ -MSH and the D-Trp<sup>5</sup> configuration that contributes to selective antagonist activities. Table 3 compares the binding affinities of the D-Trp<sup>5</sup> analogues having different constraints and extension of the C-termini, and thus, it establishes a trend toward hMC1R selectivity. Finally, the absence of Nle in the  $\gamma$ -MSH cyclized analogues leads to weak binding compared to that of the cyclized peptide with Nle (e.g., MTII), and this is consistent with our earlier findings.<sup>47</sup> Also, NMR analysis reveals a new binding site that is closely related to that of the endogenous antagonist ASIP(117–122) fragment. Table 7 illustrates the nanomolar binding affinity of this peptide toward melanoma cells (A375) that may be very useful for therapeutics.

## CONCLUSIONS

SAR and conformational studies of novel cyclized  $\gamma$ -MSH analogues have identified a highly selective hMC1R antagonist



(analogue 6). NMR studies of this constrained peptide reveal a new binding site, -D-Trp<sup>5</sup>-Cys<sup>6</sup>-Asp<sup>7</sup>-Arg<sup>8</sup>-Phe<sup>9</sup>-Gly<sup>10</sup>-, of peptide 6, which is different from the more general -His-D-Phe-Arg-Trp-pharmacophore of melanocortin receptor agonists. The backbone conformation of peptide 6 matches well with the endogenous antagonist conformation of the hMC1R selective ASIP(117–122) fragment. In this new binding site, D-Trp<sup>5</sup> and Phe<sup>9</sup> of peptide 6 play a critical role in hMC1R antagonist activity and residue D-Trp<sup>5</sup> is also crucial for binding to the sixth transmembrane domain of hMC1R.<sup>56</sup> The newly developed selective melanotropin peptides will facilitate the elucidation of the physiological roles of the hMC1R in pigmentation and immune response-related disorders. Finally, the nanomolar binding affinity of this peptide toward melanoma cells indicates that it can be used as a molecular probe for the diagnosis and treatment of skin cancer. Furthermore, the backbone conformation of peptide 6 can be used for future melanoma inhibitor discovery.

## ■ ASSOCIATED CONTENT

### ■ Supporting Information

High-resolution mass spectra of peptide analogues and extensive two-dimensional NMR spectra of peptide 6 that provide data needed for conformational analysis. This material is available free of charge via the Internet at <http://pubs.acs.org>.

## ■ AUTHOR INFORMATION

### Corresponding Author

\*Phone: (520) 621-6332. Fax: (520) 621-8407. E-mail: [hruby@email.arizona.edu](mailto:hruby@email.arizona.edu).

### Present Address

<sup>†</sup>Sanofi-Aventis, 1580 E. Hanley Blvd., Tucson, AZ 85737.

### Funding

This work was supported in part by grants from the U.S. Public Health Service, National Institutes of Health (DK17420 and DA06284).

### Notes

The authors declare no competing financial interest.

## ■ ABBREVIATIONS

AAA, amino acid analysis; Boc, *tert*-butoxycarbonyl; Fmoc, fluorenylmethoxycarbonyl; Fmo, fluorenylmethyl; Bzl, benzyl; *t*Bu, *tert*-butyl; CH<sub>3</sub>CN, acetonitrile; DCM, dichloromethane; DIEA, diisopropylethylamine; DMF, *N,N*-dimethylformamide; DIC, diisopropylcarbodiimide; HOBt, *N*-hydroxybenzotriazole; BOP reagent, benzotriazolyloxy tris(dimethylamino)-phosphonium hexafluorophosphate; Nal(2'), 2'-naphthylalanine; TFA, trifluoroacetic acid; TIPS, triisopropylsilyl; SPPS, solid-phase peptide synthesis; RP-HPLC, reverse-phase high-performance liquid chromatography; hMC1R, human melanocortin 1 receptor;  $\alpha$ -MSH, Ac-Ser-Tyr-Ser-Met-Glu-His-Phe-Arg-Trp-Gly-Lys-Pro-Val-NH<sub>2</sub>; NDP- $\alpha$ -MSH, Ac-Ser-Tyr-Ser-Nle-Glu-His-D-Phe-Arg-Trp-Gly-Lys-Pro-Val-NH<sub>2</sub>;  $\gamma$ -MSH, H-Tyr-Val-Met-Gly-His-Phe-Arg-Trp-Asp-Arg-Phe-Gly-OH; ASIP(117–122), agouti signal protein fragment.

## ■ REFERENCES

- (1) Denning-Kendall, P. A., Sumpter, J. P., and Lowry, P. J. (1982) Peptide derived from pro-opiomelanocortin in the pituitary gland of the dogfish, *Squalus acanthias*. *J. Endocrinol.* 93, 381–390.
- (2) Tatjana, H., Janis, K., Akiyoshi, K., Maja, L., Aneta, R., Johan, E., Hiroshi, K., Earl, L. T., Robert, F., and Helgi, S. B. (2007) Functional characterization of two melanocortin (MC) receptors in lamprey

showing orthology to the MC1 and MC4 receptor subtypes. *BMC Evol. Biol.* 7, 101.

- (3) Krieger, D. T., and Ganong, W. F., Eds. (1977) *ACTH and Related Peptides: Structure, Regulation, and Action*, Vol. 297, p 664, New York Academy of Sciences, New York.

- (4) Vandry, H., and Eberle, A. N., Eds. (1993) *The Melanotropic Peptides*, Vol. 680, p 687, New York Academy of Sciences, New York.

- (5) Montjoy, K. G., Robins, L. S., Mortrue, M. T., and Cone, R. D. (1992) The Cloning of a Family of Genes that Encode the Melanotropin Receptors. *Science* 257, 1248–1251.

- (6) Chhajlani, V., and Wikberg, J. E. S. (1992) Molecular cloning and expression of the human melanocyte stimulating hormone receptor cDNA. *FEBS Lett.* 309 (3), 417–420.

- (7) Gantz, I., Konda, Y., Tashiro, T., Shimoto, Y., Miwa, H., Munzert, G., Watson, S. J., DelValle, J., and Yamada, T. T. (1993) Molecular cloning of a novel melanocortin receptor. *J. Biol. Chem.* 268, 8246–8250.

- (8) Gantz, I., Miwa, H., Konda, Y., Shimoto, Y., Tashiro, T., Watson, S. J., DelValle, J., and Yamada, T. (1993) Molecular cloning, expression, and gene localization of a fourth melanocortin receptor. *J. Biol. Chem.* 268, 15174–15179.

- (9) Gantz, I., Tashiro, T., Barcroft, C., Konda, Y., Shimoto, Y., Miwa, H., Glover, T., Munzert, G., and Yamada, T. (1993) Localization of the genes encoding the melanocortin-2 (adrenocorticotrophic hormone) and melanocortin-3 receptors to chromosomes 18p11.2 and 20q13.2-q13.3 by fluorescence in situ hybridization. *Genomics. J. Biol. Chem.* 18, 166–167.

- (10) Gantz, I., Shimoto, Y., Konda, Y., Miwa, H., Dickinson, C. J., and Yamada, T. (1994) Molecular cloning, expression, and characterization of a fifth melanocortin receptor. *Biochem. Biophys. Res. Commun.* 200 (3), 1214–1220.

- (11) Cone, R. D., Ed. (2000) *The Melanocortin Receptors*, pp 1–551, Humana Press, Totowa, NJ.

- (12) *The Melanocortin System* (2003) Vol. 994, pp 1–367, New York Academy of Sciences, New York.

- (13) Hadley, M. E., Ed. (1989) *The Melanotropin Peptides*, Chapters 1–3, CRC Press, Boca Raton, FL. Eberle, A. N., and Karger, B. (1988) *The Melanotropins: Chemistry, Physiology and Mechanisms of Action*.

- (14) Roselli-Rehffuss, L., Montjoy, K. G., Robbins, L. S., Mortrud, M. T., Low, M. J., Tatro, M. L., Entwistle, M. L., Simerly, R. B., and Cone, R. D. (1993) Identification of a Receptor for  $\alpha$ -Melanotropin and Other Proopiomelanocortin Peptides in the Hypothalamus and Limbic Systems. *Proc. Natl. Acad. Sci. U.S.A.* 90, 8856–8860.

- (15) Xia, Y., Wikberg, J., and Chhajlani, V. (1995) Expression of melanocortin 1 receptors in periaqueductal gray matter. *NeuroReport* 6, 2193–2196.

- (16) Liem, E., Joiner, T., Tsueda, K., and Sessler, D. (2005) Increased sensitivity to thermal pain and reduced subcutaneous lidocaine efficacy in redheads. *Anesthesiology* 102, 509–514.

- (17) Mogil, J. S., Wilson, S. M., Chesler, E. J., Rankin, A. L., Nemmani, K. V. S., Lariviere, W. R., Groce, M. K., Wallace, A. R., Kaplan, L., Staud, R., Ness, T. J., Clover, T. L., Stakova, M., Mayorov, A., Hruby, V. J., Grisel, J. E., and Fillingim, R. B. (2003) The melanocortin-1 receptor gene mediates female-specific mechanisms of analgesia in mice and humans. *Proc. Natl. Acad. Sci. U.S.A.* 100, 4867–4872.

- (18) Hruby, V. J., Al-Obeidi, F., and Kazmierski, W. (1990) Emerging approaches in the molecular design of receptor-selective peptide ligands: Conformational, topographical and dynamic considerations. *Biochem. J.* 268, 249–262.

- (19) Hruby, V. J. (2002) Designing peptide receptor agonists and antagonists. *Nat. Rev. Drug Discovery* 1 (11), 847–858.

- (20) Hruby, V. J., Cai, M., Grieco, P., Han, G., Kavarana, M., and Trivedi, D. (2003) Exploring the stereostructural requirements of peptide ligands for the melanocortin receptors. *Ann. N.Y. Acad. Sci.* 994, 12–20.

- (21) Hruby, V. J., Smith, C. W., Bower, S. A., and Hadley, M. E. (1972) Melanophore Stimulating Hormone: Release inhibition by ring structures of neurohypophyseal hormones. *Science* 176, 1331–1332.



- (22) Hruby, V. J., Wilkes, B. C., Hadley, M. E., Al-Obeidi, F., Sawyer, T. K., Staples, D. J., de Vaux, A. E., Dym, O., de Lauro Castrucci, A.-M., Hintz, M. F., Riehm, J. R., and Rao, R. R. (1987)  $\alpha$ -Melanotropin: The Minimum Active Sequence in the Frog Skin Bioassay. *J. Med. Chem.* 30, 2126–2130.
- (23) de Lauro Castrucci, A.-M., Hadley, M. E., Sawyer, T. K., Wilkes, B. C., Al-Obeidi, F., Staples, D. J., de Vaux, A. E., Dym, O., Hintz, M. F., Riehm, J. P., Rao, R. R., and Hruby, V. J. (1989)  $\alpha$ -Melanotropin: The Minimal Active Sequence in the Lizard Skin Bioassay. *General and Comparative Endocrinology* 73, 157–163.
- (24) Grieco, P., Balse, P. M., Weinberg, D., MacNeil, T., and Hruby, V. J. (2000) D-Amino Acid Scan of  $\gamma$ -Melanocyte-Stimulating Hormone: Importance of Trp<sup>8</sup> on Human MC3 Receptor Selectivity. *J. Med. Chem.* 43, 4998–5002.
- (25) Grieco, P., Balse-Srinivasan, P., Han, G., Weinberg, D., MacNeil, T., Van der Ploeg, L. H. T., and Hruby, V. J. (2002) Synthesis and Biological Evaluation on hMC3, hMC4 and hMC5 Receptors of  $\gamma$ -MSH Analogs Substituted with L-Alanine. *J. Pept. Res.* 59, 203–210.
- (26) Cai, M., Nyberg, J., and Hruby, V. J. (2009) Melanotropins as Drugs for the Treatment of Obesity and Other Feeding Disorders: Potential and Problems. *Curr. Top. Med. Chem.* 9, 554–563.
- (27) Hruby, V. J., Cai, M., Nyberg, J., and Muthu, D. (2011) Approaches to the Rational Design of Selective Melanocortin Receptor Antagonists. *Expert Opin. Drug Discovery* 6, 543–557.
- (28) Doedens, L., Opperer, F., Cai, M., Beck, J. G., Dedek, M., Palmer, E., Hruby, V. J., and Kessler, H. (2010) Multiple N-methylation of MT-II backbone amide bonds leads to melanocortin receptor subtype hMC1R selectivity: Pharmacological and conformational studies. *J. Am. Chem. Soc.* 132, 8115–8128.
- (29) McNulty, J. C., Jackson, P. J., Thompson, D. A., Chai, B., Gantz, L., Barsh, G. S., Dawson, P. E., and Millhauser, G. L. (2005) Structures of the Agouti Signaling Protein. *J. Mol. Biol.* 346 (4), 1059–1070.
- (30) Lebl, M., and Hruby, V. J. (1984) Synthesis of cyclic peptides by solid-phase methodology. *Tetrahedron Lett.* 25, 2067–2068.
- (31) Krchnak, V., Vagner, J., and Lebl, M. (1988) Noninvasive monitoring of solid-phase peptide synthesis by acid-base indicator. *Int. J. Pept. Protein Res.* 32, 415–416.
- (32) Polinsky, A., Cooney, M. G., Toy-Palmer, A., Osapay, G., and Goodman, M. (1992) Synthesis and conformational properties of the lanthionine-bridged opioid peptide [D-Ala<sup>2</sup>,Ala<sup>5</sup>]enkephalin as determined by NMR and computer simulations. *J. Med. Chem.* 35, 4185–4194.
- (33) Mayer, J. P., Heil, J. R., Zhang, J., and Munson, M. C. (1995) An alternative solid-phase approach to C<sub>1</sub>-oxytocin. *Tetrahedron Lett.* 36, 7387–7390.
- (34) Mosberg, H. I., and Omnaas, J. R. (1985) Dithioether-containing cyclic peptides. *J. Am. Chem. Soc.* 107, 2986–2987.
- (35) Kataoka, T., Beusen, D. D., Clark, J. D., Yodo, M., and Marshall, G. R. (1992) The utility of side-chain cyclization in determining the receptor-bound conformation of peptides: Cyclic tripeptides and angiotensin II. *Biopolymers* 32, 1519–1533.
- (36) Hruby, V. J., and Bonner, G. G. (1994) Design of novel synthetic peptides including cyclic conformationally and topographically constrained analogs. *Methods Mol. Biol.* 35, 201–240.
- (37) Jung, G. (1991) Lantibiotics: Ribosomally synthesized biologically active polypeptides containing sulfide bridges and  $\alpha$ -dihydroamino acids. *Angew. Chem., Int. Ed.* 30, 1051–1068.
- (38) Jack, R. W., and Sahl, H. G. (1995) Unique peptide modifications involved in the biosynthesis of lantibiotics. *Trends Biotechnol.* 13, 269–278.
- (39) Sahl, H. G., Jack, R. W., and Bierbaum, G. (1995) Biosynthesis and biological activities of lantibiotics with unique post-translational modifications. *Eur. J. Biochem.* 230, 827–853.
- (40) Kaiser, E., Colescott, R. L., Bossinger, C. D., and Cook, P. I. (1970) Color test for detection of free terminal amino groups in the solid-phase synthesis of peptides. *Anal. Biochem.* 34, 595–598.
- (41) Al-Obeidi, F., Hadley, M. E., Pettitt, B. M., and Hruby, V. J. (1989) Design of a new class of superpotent  $\alpha$ -melanotropins based on quenched dynamic simulations. *J. Am. Chem. Soc.* 111, 3413–3416.
- (42) Al-Obeidi, F., Castrucci, A. M. L., Hadley, M. E., and Hruby, V. J. (1989) Potent and prolonged acting cyclic lactam analogues of  $\alpha$ -melanotropin: Design based on molecular dynamics. *J. Med. Chem.* 32, 2555–2561.
- (43) Hruby, V. J., Lu, D., Sharma, S. D., Castrucci, A. M. L., Kesterson, R., Al-Obeidi, F., Hadley, M. E., and Cone, R. D. (1995) Cyclic lactam  $\alpha$ -melanotropin analogues of Ac-Nle<sup>4</sup>-cyclo[Asp<sup>5</sup>,D-Phe<sup>7</sup>,Lys<sup>10</sup>]  $\alpha$ -melanocyte-stimulating hormone-(4–10)-NH<sub>2</sub> with bulky aromatic amino acids at position 7 show high antagonist potency and selectivity at specific melanocortin receptors. *J. Med. Chem.* 38, 3454–3461.
- (44) Sawyer, T. K., Sanfilippo, P. J., Hruby, V. J., Engel, M. H., Heward, C. B., Burnett, J. B., and Hadley, M. E. (1980) 4-Norleucine, 7-D-phenylalanine- $\alpha$ -melanocyte-stimulating hormone: A highly potent  $\alpha$ -melanotropin with ultralong biological activity. *Proc. Natl. Acad. Sci. U.S.A.* 77, 5754–5758.
- (45) Grieco, P., Balse, P. M., Weinberg, D., MacNeil, T., and Hruby, V. J. (2000) D-Amino acid scan of  $\gamma$ -melanocyte-stimulating hormone: Importance of Trp(8) on human MC3 receptor selectivity. *J. Med. Chem.* 43, 4998–5002.
- (46) Cai, M., Mayorov, A. V., Cabello, C., Stankova, M., Trivedi, D., and Hruby, V. J. (2005) Novel 3D Pharmacophore of  $\alpha$ -MSH/ $\gamma$ -MSH Hybrids Leads to Selective Human MC1R and MC3R Analogues. *J. Med. Chem.* 48, 1839–1848.
- (47) Cai, M., Cai, C., Mayorov, A. V., Xiong, C., Cabello, C. M., Soloshonok, V. A., Swift, J. R., Trivedi, D., and Hruby, V. J. (2004) Biological and conformational study of  $\beta$ -substituted prolines in MT-II template: Steric effects leading to human MC5 receptor selectivity. *J. Pept. Res.* 63 (2), 116–131.
- (48) Wüthrich, K., Billeter, M., and Braun, W. (1984) Polypeptide secondary structure determination by nuclear magnetic resonance observation of short proton-proton distances. *J. Mol. Biol.* 180, 715–740.
- (49) Williamson, M. P., and Waltho, J. (1984) Peptide structure from NMR. *Chem. Soc. Rev.* 21, 227–236.
- (50) Cierpicki, T., and Otlewski, J. (2001) Amide proton temperature coefficients as hydrogen bond indicators in proteins. *J. Biomol. NMR* 21, 249–261.
- (51) Wishart, D. S., Sykes, B. D., and Richards, F. M. (1992) The chemical shift index: A fast and simple method for the assignment of protein secondary structure through NMR spectroscopy. *Biochemistry* 31, 1647–1651.
- (52) Ramachandran, G. N., Ramakrishnan, C., and Sasisekharan, V. (1963) Stereochemistry of polypeptide chain configurations. *J. Mol. Biol.* 7, 95–99.
- (53) Ying, J., Koeber, K. E., Gu, X., Han, G., Trivedi, D. B., Kavarana, M. J., and Hruby, V. J. (2003) Solution structures of cyclic melanocortin agonists and antagonists by NMR. *Biopolymers* 71, 696–716.
- (54) Grieco, P., Lavecchia, A., Cai, M., Trivedi, D., Weinberg, D., MacNeil, T., Van der Ploeg, L. H., and Hruby, V. J. (2002) Structure-activity studies of the melanocortin peptides: Discovery of potent and selective antagonists at MC3 and MC4 receptors. *J. Med. Chem.* 45, 5287–5294.
- (55) Patel, M. P., Cribb Fabersunne, C. S., Yang, Y., Kaelin, C. B., Barsh, G. S., and Millhauser, G. L. (2010) Loop-swapped chimeras of the Agouti-Related Protein and the Agouti Signaling Protein identify contacts required for Melanocortin 1 Receptor selectivity and antagonism. *J. Mol. Biol.* 404, 45–55.
- (56) Chen, M., Cai, M., McPherson, D., Hruby, V. J., Harmon, C. M., and Yang, Y. (2009) Contribution of the transmembrane domain 6 of melanocortin-4 receptor to peptide [Pro<sup>5</sup>,D<sup>8</sup>Nal(2′)8]- $\gamma$ -MSH selectivity. *Biochem. Pharmacol.* 77, 114–124.
- (57) Gudbjartsson, D. F., Sulem, P., Stacey, S. N., Goldstein, A. M., Rafnar, T., Sigurgeirsson, B., Benediktsson, K. R., Thorisdottir, K., Ragnarsson, R., Sveinsdottir, S. G., et al. (2008) ASIP and TYR pigmentation variants associate with cutaneous melanoma and basal cell carcinoma. *Nat. Genet.* 40 (7), 886–891.



(58) Mayorov, A. V., Cai, M., Palmer, E. S., Liu, Z., Cain, J. P., Vagner, J., Trivedi, D., and Hruby, V. J. (2010) Solid-Phase Peptide Head-to-Side Chain Cyclodimerization: Discovery of C<sub>2</sub>-Symmetric Cyclic Lactam Hybrid  $\alpha$ -Melanocyte-Stimulating Hormone (MSH)/Agouti-Signaling Protein (ASIP) Analogues with Potent Activities at the Human Melanocortin Receptors. *Peptides* 31 (10), 1894–1905.